

Gamow-Teller strength at high excitations

G. F. Bertsch and I. Hamamoto*

Cyclotron Laboratory, Michigan State University, East Lansing, Michigan 48824

(Received 14 May 1982)

A perturbative calculation is reported for the mixing of Gamow-Teller strength with two-particle two-hole configurations at high excitation energies. We find that roughly 50% of the Gamow-Teller strength is shifted into the region of 10–45 MeV excitation for the nucleus ^{90}Zr . This would explain a substantial part of the continuum background seen in the 200 MeV (p, n) reaction.

[NUCLEAR STRUCTURE ^{90}Zr , Gamow-Teller strength function,
 $E_{\text{ex}} = 10\text{--}45$ MeV, theory.]

The recent elucidation of the giant Gamow-Teller state in heavy nuclei by the (p, n) reactions presents a paradox. There is a well-defined peak whose energetics is reproduced by the Tamm-Dancoff approximation (TDA) shell model theory,¹ but the strength is apparently less than half of the predicted value.^{2,3} Part of the suppression can be ascribed to the Δ -isobar admixtures in the nuclear wave functions,^{4–6} but part is undoubtedly due to conventional nuclear mixing.^{6,7} For example in the case of ^{41}Sc , Towner and Khanna⁶ found that more strength was depleted by ordinary nuclear configuration mixing than by the Δ amplitudes in the wave functions.

In this article, we will examine in some detail the distribution of the strength that is lost to the Gamow-Teller peak due to configuration mixing. Our motivation is the presence of excitation strength in the (p, n) reaction at 0° , for excitation energies ranging up to ~ 50 MeV above the Gamow-Teller peak.³ We anticipate that much of this excitation strength is due to Gamow-Teller strength for the following reasons. The main other possibilities are multistep excitation, and excitation by operators with orbital dependence, e.g., $[Y_L(r)\sigma\tau]_J$. Multistep reaction cross sections characteristically rise with increasing excitation energy, due to the greater number of intermediate states possible for higher energy losses. However, the (p, n) reaction cross section falls with energy loss up to excitation energies beyond 50 MeV. This is clearly seen in the data of Gaarde *et al.*,³ which we reproduce in Fig. 1. Furthermore, explicit calculation of multistep reaction cross sections indicates that single step should dominate at forward angles when the excitation energy is less than half the beam energy.⁸ Concerning the possibility of single-step excitation with $L \neq 0$, we note that distorted-wave impulse approximation (DWIA) calculations of angular distributions predict that the 200 MeV (p, n) cross section increases with angle for all multipoles but $L = 0$. The experimental angular distribution in

the continuum region⁹ is flat near 0° , indicating that $L \neq 0$ cannot dominate the 0° cross section. A model calculation of the continuum cross section which assumed no Gamow-Teller strength in this region, failed to reproduce the 0° continuum cross section by a factor of 3, while agreeing at larger angles.¹⁰ In contrast to the (p, n) results, the model fit the angular distribution of the (p, p') reaction quite well, down to the lowest angles measured. More microscopic calculations of the continuum region have been made by Osterfeld,¹¹ who also finds that $L \neq 0$ multipoles are insufficient to explain the 0° cross section. The angular distribution⁸ between 0° and 10° can be well fit as a sum of $L = 0, 1$ and 2 multipoles.¹² According to the fit, roughly half of the 0° cross section for $^{90}\text{Zr}(p, n)$ at 30 MeV excitation energy is due to $L = 0$.

Our calculation of the Gamow-Teller strength in the continuum will be based on second-order pertur-

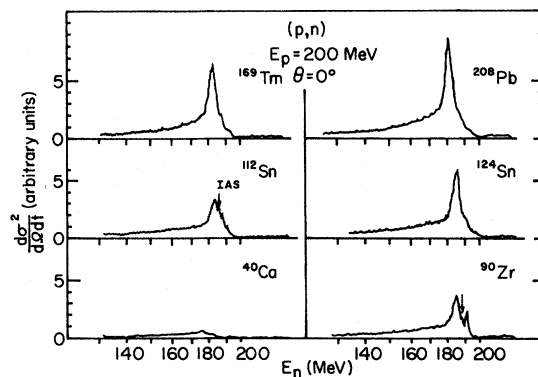


FIG. 1. Differential cross section for the (p, n) reaction at 200 MeV and 0° scattering angle, from Gaarde *et al.* (Ref. 3). Note the long tail at excitation energies above the Gamow-Teller peak, which is present only in the nuclei with neutron excesses.

bation theory, using the best model of the nuclear interaction at our disposal. At the most naive level, we anticipate the outcome of the calculation by the second-order perturbation effects on the single-particle wave functions. We know that the single-particle probability is reduced by about 25% by correlations, and so we could expect a 50% reduction of Gamow-Teller strength from the graphs shown in Figs. 2(a) and 2(b). This strength would be shifted to the continuum region extending up to ~ 200 MeV, with the tensor correlations responsible for the highest energy components.

The actual shift in strength may differ substantially from the predictions of this argument for the following reason. There are other graphs which contribute in the same order in the interaction to the strength function, one of which is shown in Fig. 2(c). These ground state correlation graphs are coherent with the graphs of Figs. 2(a) and 2(b) and therefore all must be calculated together. Whether the ground state correlations interfere constructively or destructively with the final state correlations depends on the nature of the excitation operator and the residual interaction. For scalar excitations, the effect of the ground state correlations is to suppress the transfer of strength to higher energies, i.e., the strength distribution tends to be unaffected by the presence of correlations. This may be illustrated schematically with a one-particle model, in which the operator transfers a large amount of energy compared to the momentum transferred. Then the perturbation amplitude of the matrix element to a high energy state involves the sum

$$a = \sum_{p''} \frac{\langle p' | v | p'' \rangle \langle p'' | \Theta | p \rangle}{E - E_{p''} + E_p} + \sum_{p'''} \frac{\langle p' | \Theta | p''' \rangle \langle p''' | v | p \rangle}{-E_{p'''} + E_p}, \quad (1)$$

where $|p\rangle$ is the initial state, $|p'\rangle$ the final state, Θ is the excitation operator, and E is the energy transferred by the operator. The energy of the final state is $E_{p'} = E + E_p$. The condition of low momentum transfer by the operators requires that $p'' \approx p$ and $p''' \approx p'$. Using this to replace the denominators

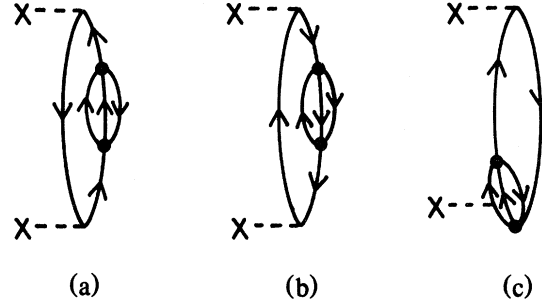


FIG. 2. Perturbative graphs to calculate the strength function for an operator at high excitation energies. Graphs (a) and (b) represent final state interactions of the particle and hole. Graph (c) is an example of ground state correlation amplitudes interfering with a final state interaction.

$E - E_{p''} + E_p \approx E$ and $E_{p'''} - E_p \approx +E$, we see that the denominators are equal and opposite. Thus the amplitude is proportional to the commutator of the potential and the excitation operator.

$$a \approx \frac{\langle p' | [V, \Theta] | p \rangle}{E}. \quad (2)$$

Operators that are spin- and isospin-scalars commute with the potential, and thus the high energy strength is small. However, the Gamow-Teller operator $\sigma\tau$ does not commute with the nuclear interaction, particularly the tensor interaction. We thus do not expect as much of a cancellation between final state and ground state correlation amplitudes; it is even possible that they add coherently.

We study the nucleus ^{90}Zr , with the following Hamiltonian. The single-particle wave functions are eigenstates of a Woods-Saxon potential, in which the continuum has been discretized by demanding that the wave functions vanish at $r = 12$ fm. This causes some unphysical structure in the continuum function, so only the average predicted strength will have significance. The residual interaction was chosen with S -wave components given by the Reid soft-core effective interaction of Ref. 13. This interaction is based on a Yukawa fit to the Brueckner G matrix, with a long-range part identical to a one-pion-exchange potential (OPEP). We neglect the odd partial waves and express the interaction in momentum space as

$$V_c(q) = \left(\frac{f}{m_\pi} \right)^2 \left[\frac{1}{3} \sigma_1 \cdot \sigma_2 \tau_1 \cdot \tau_2 \frac{m_\pi^2}{q^2 + m_\pi^2} + (-4.24 + 0.66 \sigma_1 \cdot \sigma_2 + 2.17 \tau_1 \cdot \tau_2 + 1.41 \sigma_1 \cdot \sigma_2 \tau_1 \cdot \tau_2) \frac{m_a^2}{q^2 + m_a^2} + (3.33 - 0.53 \sigma_1 \cdot \sigma_2 - 1.69 \tau_1 \cdot \tau_2 - 1.11 \sigma_1 \cdot \tau_2 \tau_1 \cdot \tau_2) \frac{m_b^2}{q^2 + m_b^2} \right], \quad (2)$$

where $f = 0.97$, $m_a = 2.5 \text{ fm}^{-1}$, and $m_b = 4 \text{ fm}^{-1}$. We take the tensor interaction to have the same form, fit to the Reid soft-core G -matrix elements of Ref. 13. Unlike the central interaction, the tensor interaction can be well

fit with a two-term Yukawa. The fit is insensitive to the range of the short-range term, and we have taken

$$V_T(q) = - \left(\frac{f}{m_\pi} \right)^2 \frac{\tau \cdot \tau}{3} (3\sigma_1 \cdot q \sigma_2 \cdot q - \sigma_1 \cdot \sigma_2 q^2) \times \left(\frac{1}{m_\pi^2 + q^2} - \frac{0.89}{m_a^2 + q^2} \right). \quad (3)$$

Both direct and exchange matrix elements of the interaction must be included to reproduce the G -matrix elements. The matrix elements between shell model states are computed in momentum space, using the formulas of Ref. 14. [The equation following (A1) in Ref. 14, for $a_{LL'}$, should include a phase $(-1)^{(L-L')/2}$.]

The strength function can be formally written as $1/\pi$ times the imaginary part of the response function, which allows one to see that the only graphs contributing to the strength function at $E = \epsilon_p + \epsilon_{p'}$, $-\epsilon_h - \epsilon_{h'}$, can be expressed as the square of the sum of the four amplitudes shown in Fig. 3. We included in the calculation all of the 2p-2h states that can be excited in Figs. 3(a) and 3(b), and only computed Figs. 3(c) and 3(d) for these states. There are roughly 20 000 states that need to be considered in the 10–45 MeV excitation energy range. In Table I the total strength for this region is tabulated, broken down by type of interaction and graph. We see that the central and tensor interactions are roughly of equal importance, and that they add incoherently to the strength. We also see that the separated ground state correlation contribution is somewhat smaller than the final states correlation contribution, and these tend to also add incoherently.

The distribution of strength with excitation energy is shown in Fig. 4. The strength function $P(E)$ is defined with a normalization of 1, i.e.,

$$P(E) = \frac{\sum_f \langle i | \sigma \tau_- | f \rangle^2 \delta(E - E_{if})}{\sum_f \langle i | \sigma \tau_- | f \rangle^2}. \quad (4)$$

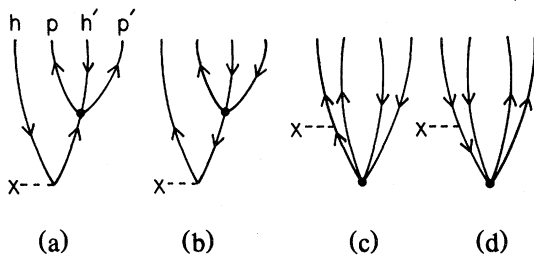


FIG. 3. Four types of amplitude included in the actual calculation. (a) should of course also include the graph with h and h' interchanged.

TABLE I. Contributions to Gamow-Teller strength in the region 10–45 MeV excitation in ^{90}Zr , $\int_{10}^{45} P(E) dE$, with $P(E)$ defined in Eq. (4). The partial sums need not add to the total because of possible coherence of amplitudes.

$\int P$	Graphs (a) + (b)	Graphs (c) + (d)	Total
Tensor	0.13	0.06	0.20
Central	0.25	0.15	0.36
Total	0.38	0.20	0.56

The abscissa in Fig. 4 shows excitation energy with respect to the ground state in ^{90}Nb . The Gamow-Teller peak, which is well reproduced by TDA theory, would lie just off the figure on the left. However, our perturbative calculation does not include the collective energy shift, and so we would underestimate the strength in the region around 10 MeV excitation. If the calculated strength function were smoothed out to compensate for spreading widths and the discretized single-particle spectrum, the strength would decrease from $P \cong 0.025/\text{MeV}$ at $E \approx 10$ MeV to $P \cong 0.011/\text{MeV}$ at $E \approx 45$ MeV, with an average value

$$\bar{P} = \frac{0.56}{35} = 0.016/\text{MeV}.$$

This would make a significant background in the (p, n) reaction. According to Fig. 7 of Ref. 3, the 0° cross section for the 200 MeV (p, n) reaction should have a value of

$$\frac{d\sigma}{d\Omega} \Big|_{0^\circ}^{\text{GT}} = (5 \text{ mb/sr}) \langle i | \sigma \tau_- | f \rangle^2 = 150 \text{ mb/sr} \quad (5)$$

for ^{90}Zr . This is the full Gamow-Teller strength, assuming no Δ mixing, etc. The Q mismatch at 30 MeV excitation energy reduces this cross section by a factor 0.60. Our calculation then predicts that the

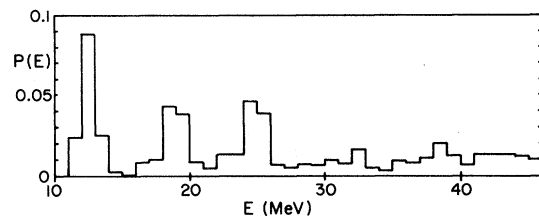


FIG. 4. Calculated strength distribution $P(E)$ for the Gamow-Teller operator in ^{90}Zr . Energies are measured with respect to the ground state of ^{90}Nb .

cross section in the upper continuum region will be

$$\frac{d^2\sigma}{d\Omega dE} = P(E) \cdot \left. \frac{d\sigma}{d\Omega} \right|_{0^+}^{\text{GT}} \approx (0.011)(0.6)(150) \\ \approx 1.0 \text{ mb/sr MeV} . \quad (6)$$

The experimental cross section⁹ at 30 MeV excitation is 2.8 mb/sr MeV. Thus the configuration mixing is strong enough to account for a substantial part of the background.

It is difficult to be more quantitative in our conclusion. Since the function $P(E)$ depends quadratically on the interaction, it is very sensitive to the assumed interaction. The G -matrix interactions are pretty well determined; newer potentials such as the Paris potential yield virtually identical G matrices.¹⁵ But the G -matrix theory itself is not completely reliable, in view of the well-known problems of saturation of nuclear matter. Also, we neglected Δ mixing, and higher order interaction effects. Some of these

effects, such as the renormalization of the strength in the Gamow-Teller state, would tend to reduce the mixing into the continuum, but other effects such as the coupling to collective vibrations would give an increased mixing.

The function $P(E)$ is expected to drop off at higher excitation energies, because the off-diagonal matrix elements of the central force decrease rapidly. Unfortunately, computer limitations restricted the present calculation to 45 MeV excitation. It would be interesting to extend the calculations to higher excitations with a simpler model, to see if the overall shape of the energy spectrum is reproduced. Finally, it would also be interesting to study the strength distribution for other operators, for example, the mass quadrupole operator, where the coherences might be different.

We would like to thank H. Toki, H. Kruse, O. Scholten, and S. Austin for helpful discussions. This work was supported by the National Science Foundation under Grant No. PHY-80-17605.

*Also at NORDITA, Copenhagen. Present address: Department of Mathematical Physics, Lunds Institute of Technology, University of Lund, S-22077 Lund 7, Sweden.

¹G. Bertsch, D. Cha, and H. Toki, Phys. Rev. C **24**, 533 (1981).

²C. Goodman, Comments Nucl. Part. Phys. **10**, 117 (1981).

³C. Gaarde *et al.*, Nucl. Phys. **A369**, 258 (1981).

⁴M. Ericson, A. Figureau, and C. Thévenet, Phys. Lett. **45B**, 19 (1973).

⁵E. Oset and M. Rho, Phys. Rev. Lett. **42**, 47 (1979).

⁶I. S. Towner and F. C. Khanna, Phys. Rev. Lett. **42**, 51 (1979).

⁷A. Arima and H. Hyuga, in *Mesons in Nuclei*, edited by D.

Wilkinson (North-Holland, Amsterdam, 1979), p. 683; K. Shimizu, M. Ichimura, and A. Arima, Nucl. Phys. **A226**, 282 (1978).

⁸H. C. Chiang and J. Hüfner, Nucl. Phys. **A349**, 466 (1980).

⁹N. Taddeucci (private communication), quoted in Ref. 10 below.

¹⁰G. Bertsch and O. Scholten, Phys. Rev. C **25**, 804 (1982).

¹¹F. Osterfeld (unpublished).

¹²O. Scholten (private communication).

¹³G. Bertsch, J. Borysowicz, H. McManus, and W. G. Love, Nucl. Phys. **A284**, 399 (1977).

¹⁴J. Meyer-ter-Vehn, Phys. Rep. **74**, 323 (1981).

¹⁵N. Anantaraman (private communication).